JOURNAL OF THERMOPHYSICS AND HEAT TRANSFER
Vol. 9, No. 4, October–December 1995

Galileo High-Gain Antenna Deployment Anomaly Thermal Analysis Support

G. Tsuyuki* and R. Reeve†
Jet Propulsion Laboratory, California Institute of Technology, Pasadena, California 91109

In April of 1991, the Galileo spacecraft executed a sequence of commands to unfurl its umbrella-like high-gain antenna, but confirmation of deployment was not received. The primary theory was that a very high coefficient of friction existed between the midrib restraint pins and their receptacles along the antenna's central tower. Recovery actions included extreme antenna cold soaking, cyclic warming and cooling of the antenna, and pulsing the deployment motors to act as a mechanical hammer. An analytical model was extensively used to quantify the benefit of these actions. This model was not primarily intended to produce accurate temperatures in extremely cold environments. Initially, predicted antenna temperatures for cold soaking were different by as much as 40°C. However, with additional flight experience, this difference was reduced to within 20°C. Good agreement (within 5°C) with flight data was achieved for antenna warming and motor hammering. Although deployment was not achieved, the analytical model evolved without extensive revision into an accurate tool for predicting antenna temperatures.

Introduction

AN analytical model was extensively used to support the recovery actions. The model was initially developed to support the Venus trajectory redesign effort. It was not intended to produce adequate temperature predictions for the recovery actions. In order to provide timely support for recovery decisions, the model and previous flight experience were used to develop more accurate temperature predictions as time progressed. This approach is in stark contrast to rigorous correlation of the model with flight data as it becomes available. The purpose of this article is to describe the evolution of this alternate approach and show that it adequately supported the recovery effort. The focus will be on the antenna-related elements, therefore, no in-depth discussion is presented for the analysis of the other spacecraft components.

Hardware Description

The high-gain antenna was fabricated by the Harris Corporation and it is based on the Tracking and Data Relay Satellite antenna. The antenna is a Cassigrainian system with a gold-plated molybdenum wire mesh stretched across its 18 graphite/epoxy ribs representing the parabolic primary reflector as shown in Fig. 1. A schematic of the stowed antenna cross section is depicted in Fig. 2. The radome assembly, which includes the antenna subreflector, is positioned atop a beryllium feed-truss assembly. The plasma wave science support structure and the low-gain antenna are sequentially stacked above the radome. Each of the ribs pivots about its base. A ball screw on the centerline is driven by redundant motors, and it raises a carrier ring attached to the ball nut. Each rib is connected to the carrier ring via a pushrod. As the carrier raises, the ribs are nominally rotated into their fully deployed position. Each rib is firmly supported during launch at its midspan and tip.

Thermal Design Description

The general approach employed passive techniques in order to meet the temperature limits listed in Table 1. Galileo was launched in October 1989 and is currently on a circuitous route to Jupiter, its ultimate destination. The spacecraft is typically in a spin-stabilized mode during cruise. The cruise trajectory to Jupiter is illustrated in Fig. 3. Shortly after launch, the spacecraft headed toward Venus for the first of three planetary gravity assists, since the launch energy alone was not sufficient to reach Jupiter. In order to protect the parabolic reflector from the intense solar irradiance at Venus (~2.2 equivalent suns), the antenna remained stowed and was protected from direct insolation by a tip shade located at the base of the low-gain antenna while the spacecraft remained pointing the antenna boresight at the sun. Each of the graphite/epoxy ribs was wrapped with multilayered insulation blankets as well as the feed truss assembly. Since the radome housed the subreflector, multilayered insulation blanketing was not

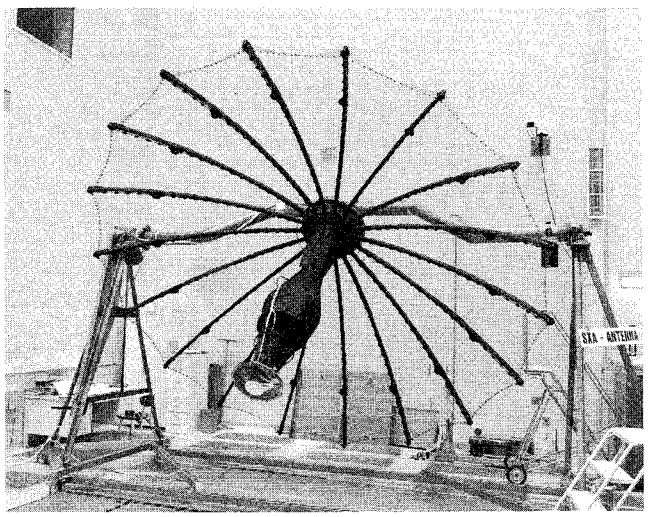

Fig. 1 Fully deployed antenna on a test fixture.

Presented as Paper 94-2003 at the AIAA/ASME 6th Joint Thermophysics and Heat Transfer Conference, Colorado Springs, CO, June 20–23, 1994; received Nov. 17, 1994; revision received May 4, 1995; accepted for publication May 8, 1995.

*Technical Group Leader, Spacecraft Thermal Engineering and Flight Operations Group, Thermal and Propulsion Engineering Section, 4800 Oak Grove Drive, M/S 301-358. Senior Member AIAA.

†Technical Group Supervisor, Spacecraft Thermal Engineering and Flight Operations Group, Thermal and Propulsion Engineering Section, 4800 Oak Grove Drive, M/S 301-358.

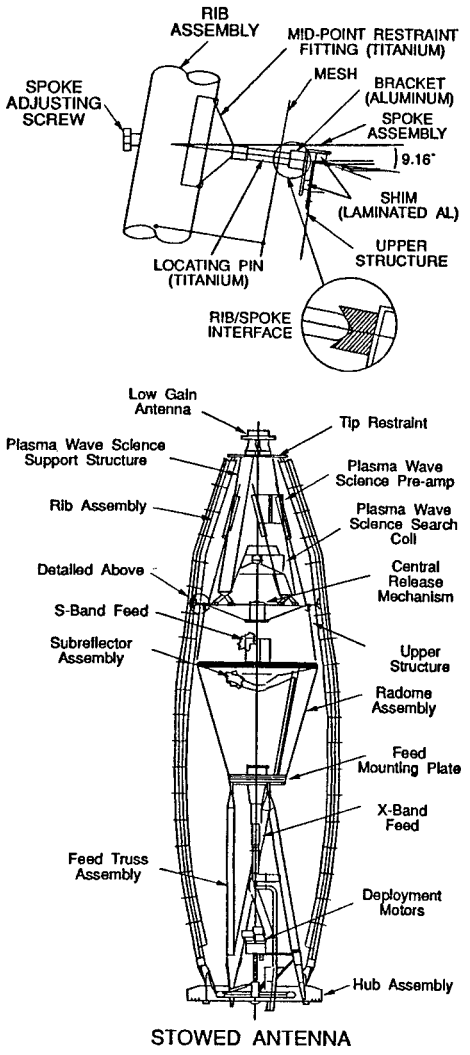

Fig. 2 Schematic of stowed antenna.

permitted since it would significantly attenuate rf signals. The plasma wave science support structure was covered by a single layer of black Kapton®. The tip shade consisted of an aluminum honeycomb structure with spokes to support the carbon-filled Kapton shade itself. The backside of the honeycomb structure was covered with zinc orthotitanate white paint and acted as a radiator for the attached low-gain antenna. The low-gain antenna was also painted with zinc orthotitanate white paint since it could not be shaded from the sun. However, the low-gain antenna base could be blanketed, and this blanketing was attached to the tip shade honeycomb structure. Behind the parabolic reflector, a large conical bus shade protected the remainder of the spacecraft from insolation (see Fig. 4). The deployment motors were conductively coupled with the spacecraft bus through the attachment structure. Through mission planning, sufficient opportunities were identified to deploy the antenna ribs when the motors were within flight allowable temperatures without the use of an electrical heater.

Deployment Anomaly

The anomaly has been well chronicled by O'Neil et al.[1,2] On April 11, 1991, the Galileo spacecraft executed a sequence of commands to unfurl its umbrella-like high-gain antenna. The initial deployment opportunity occurred at a solar distance of 1.32 astronomical unit (AU), 8 months prior to an

Table 1 Antenna flight allowable temperatures[a]

Item	Operating	Nonoperating
Reflector ribs		
Stowed	−168/113	−168/113
Deployed	−168/100	−168/100
Low-gain antenna	−200/104	−200/104
X-band feed	−92/65	−92/65
S-band feed	−156/82	−156/82
Deployment motor	−35/44	−57/55
Central release mechanism	−101/93	NA[b]
Ball screw, nut, and bearing	−29/65	−120/NA

[a]In degrees Centigrade, °C. [b]Not applicable.

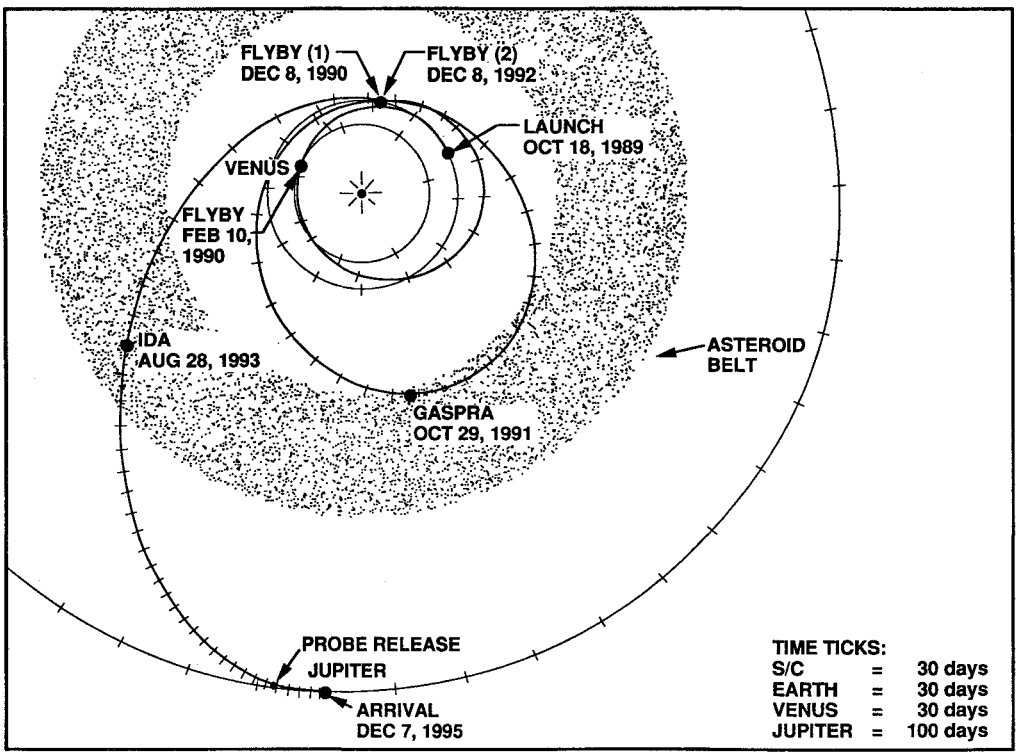

Fig. 3 Galileo trajectory to Jupiter.

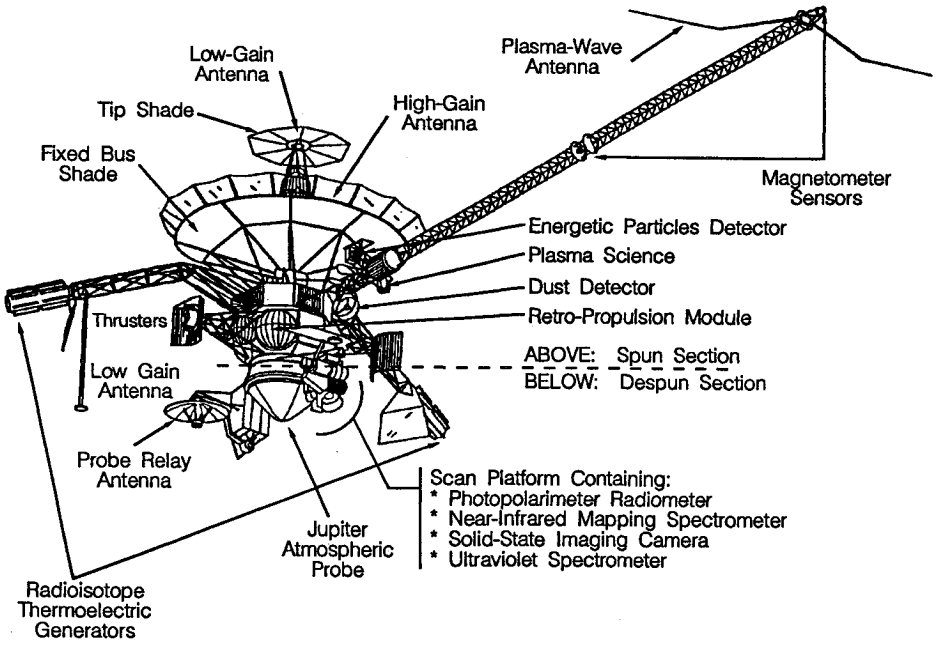

Fig. 4 Galileo spacecraft configuration.

aphelion of 2.27 AU and approximately 20 months prior to a gravity-assist from the Earth that would hurl the spacecraft toward Jupiter. Confirmation of deployment was not received. An investigation team was assembled to determine likely failure scenarios and to recommend courses of recovery actions. After intensive analysis of flight telemetry (attitude control wobble, sun gate obscuration, and deployment motor current), the team postulated that a number of the antenna's 18 ribs were stuck in the fully stowed position. Subsequent ground testing of the spare antenna was correlated to the flight telemetry, and the team concluded that probably three or four ribs were stuck in their stowed position. Investigation of the spacecraft design revealed that the forces that could be applied to the antenna were limited to 1) spinning the spacecraft faster to increase centripetal forces, 2) stowing and redeploying a boom, 3) repeated pulsing of the deployment motors to induce impulsive forces, 4) inducing spacecraft wobble, 5) firing thrusters, or 6) changing the spacecraft attitude relative to the sun to promote thermally induced forces. Efforts to free the antenna ribs solely employed actions no. 1, 2, 3, and 6.

The leading theory that emerged centered on the midrib restraints that act as braces when the ribs are stowed. Each rib is braced by a pair of "locating pins" that fit into receptacles along the tower (see Fig. 5). A spoke that is located between the pins was tensioned to 85 lb to firmly hold each rib to the tower. During ground transportation, the antenna was horizontally cantilevered from its base, and the presently stuck ribs, which were nearest the vertical plane, received the greatest vibration. In turn, this caused a loss of the dry lubricant and subsequent galling of the pin and receptacle surfaces. When the spacecraft achieved the hard vacuum of space, a very large effective coefficient of friction (~1.25) developed at the contact stress points. As the ball-screw rotation initiated during the initial deployment opportunity, flight telemetry suggests that some neighboring and some opposite ribs were held to the tower by the friction force, thus preventing their pins from sliding off the contact stress points. Deployment forces became more concentrated in the stuck ribs as deployment continued. After one ball-screw turn, the opposite stuck ribs popped free, and after three ball-screw turns, the neighboring ribs had been released (leaving three ribs stuck as shown in Fig. 6). Further ball-screw rotation caused the stuck ribs to be bowed by the bending moment applied at

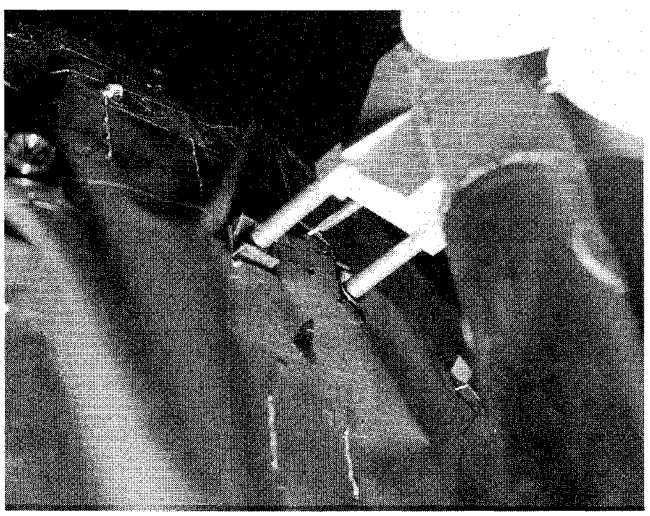

Fig. 5 Antenna mid-rib locating pins.

their base by the push rods. This caused the pins to rotate downward, thus increasing contact stress on the lower surface of the receptacles. When the deployment motors reached a full stall condition, at least one pin of each pair had driven itself into the lower surface of its receptacle. The stall occurred due to the bending moment on the ball screw resulting from the asymmetric loading of the carrier.

Extreme Antenna Cooling

Extreme cooling of the antenna was proposed to reduce the bending moment-induced stress on the receptacle lower surfaces and to transfer preload stress to the easier-sliding upper surfaces. If the cooling produced sufficient tower contraction with respect to the room temperature assembly condition, the stored strain energy in the stuck ribs would free them. The cooling was accomplished by turning the spacecraft 165 deg so that the antenna pointed to deep space, and the bus shade obstructed the sun from directly illuminating the antenna.

Prior to the turn, analytical predictions were performed with a simplified version of the high-gain antenna thermal math model, which was developed by the Harris Corporation.

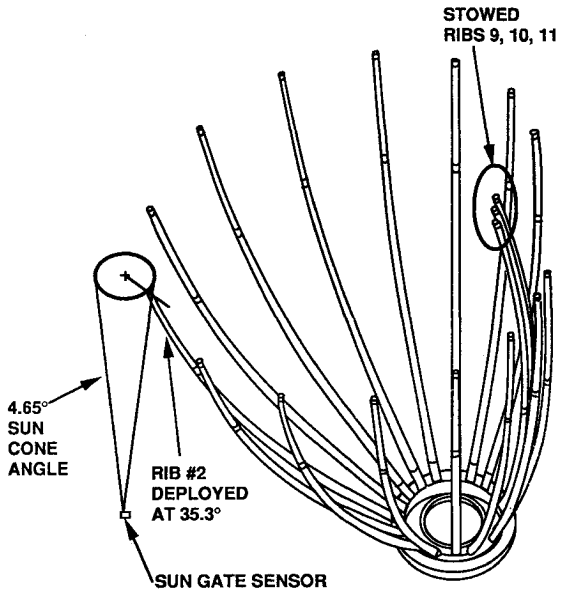

Fig. 6 Postulated antenna configuration with three stuck ribs immediately after deployment attempt.

Originally, this model was intended to support the Venus trajectory redesign effort,[3] and its use for other purposes had to be carefully considered. The thermal model is a finite difference type with a total of 71 nodes, 38 linear conductors, and 682 radiation conductors. Due to its intended purpose, the majority of the model represented "external" components such as the bus and tip shades, antenna ribs, radome, the single black Kapton layer over the plasma wave science support and upper structures, and the low-gain antenna. Limited modeling of "internal" equipment included the subreflector assembly, S-band feed, and deployment motors.

As an estimate of the model accuracy, this model was compared with data from the spacecraft solar-thermal vacuum test performed in 1985. With the antenna in an orientation that represented the nominal cruise configuration (antenna boresight pointed at the sun), two solar irradiance levels were tested: one sun (1.0 AU) and no sun (conservative Jupiter environment). The tower cavity created by the multilayered insulation blanket wrapping of the feed truss assembly demonstrated very good agreement with test data (within 5°C for one sun and within 10°C for no sun). The radome area exhibited satisfactory agreement with the test (within 20°C for both conditions). However, the low-gain antenna demonstrated the poorest agreement with the test (within 40°C for both conditions). This was attributed to the single lumped node modeling assumption of low-gain antenna that was deemed too simplistic. However, the low-gain antenna temperature was not a significant factor in assessing the benefit of any recovery action.

Extensive revisions of the model were not undertaken so that responses would be timely. Instead, a bounding analysis for the first cooling turn was performed to determine antenna temperature extremes. The worst-case cold temperatures were determined by removing the sun-pointed environmental heating. On the other hand, the worst-case hot temperatures were computed by setting the bus shade as a boundary temperature. This boundary was determined from the spacecraft solar-thermal vacuum test data for the nonilluminated side of the bus shade in the 1.0 AU sun-pointed condition. Premaneuver tower spatial temperature predictions are shown in Fig. 7 (predictions will be considered as direct results from the model, whereas estimates refer to calculations resulting from applying any judgment to predictions).

A simple one-dimensional thermal contraction model was developed. The total tower contraction was determined as the

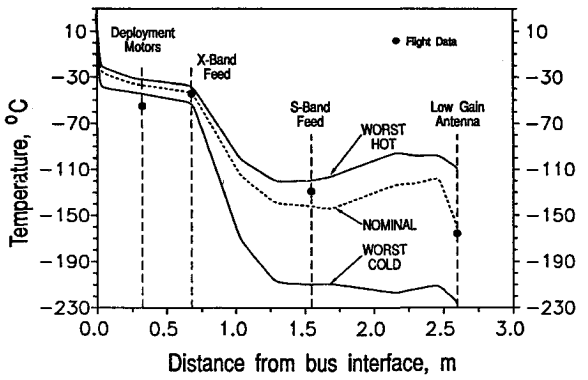

Fig. 7 Cooling turn no. 1 bounding tower temperature predictions and flight data.

sum of linear thermal displacements of each tower element from the antenna hub to the central release mechanism. The temperature difference driving the thermal contraction was calculated from 20°C, since it was assumed that there was no pin preload when the antenna was assembled at room temperature. Since the thermal math model did not explicitly represent all the elements in the contraction model, certain interpolations of the temperature predictions were required. Spacecraft solar-thermal vacuum test data was used either to verify or assist in the formulation of interpolation expressions. Using the thermal math model temperatures, tower contraction was bounded between 1.50–2.34 mm, and rib release appeared possible.

The first cooling turn was performed on July 10, 1991 at a heliocentric distance of 1.84 AU. The total duration at attitude, 32 h, was constrained by the illumination of spacecraft components such as the Probe that were never intended to be sunlit. However, flight data indicated that steady state was nearly achieved, although none of the stuck ribs released. There are four temperature sensors on the high-gain antenna: 1) on a deployment motor support, 2) X-band feed, 3) S-band feed, and 4) low-gain antenna. Flight data from these sensors indicated that the antenna tower temperature was more in agreement with the predicted worst-case hot temperature levels (see Fig. 7). The resolution of flight temperature measurements is ±0.7°C. Following the first cooling turn, the flight tower temperature profile was approximated by varying the bus shade boundary temperature of the analytical model as a function of the square of the heliocentric distance until better agreement with flight data was obtained. These temperature estimates were inserted into the tower contraction model and calculations suggest that between 1.73 ± 0.01 mm of contraction was actually attained. This range was obtained by utilizing the measurement error of the flight temperature sensors.

During the first turn, a 3-W thermostatically controlled heater was active on the plasma wave science preamplifier in order to maintain acceptable temperatures. Further investigative work revealed that this heater power dissipation could be responsible for the warmer than expected midtower temperatures. Again, a bounding thermal analysis was performed. The results suggested that an additional 0.11–0.28 mm of contraction (a tower contraction range between 1.83–2.02 mm) could be obtained if the plasma wave science search coil preamplifier heater was completely turned off. However, a peer review board remained skeptical that such a relatively large benefit would be realized. A second cooling turn was performed on Aug. 12, 1991 at a heliocentric distance of 1.98 AU, since the prior actual tower contraction appeared to be close to what might cause rib release. Thermal model refinements such as empirical determination of the bus shade temperature and more realistic modeling of the plasma wave science preamplifier heater were used to determine more accurate

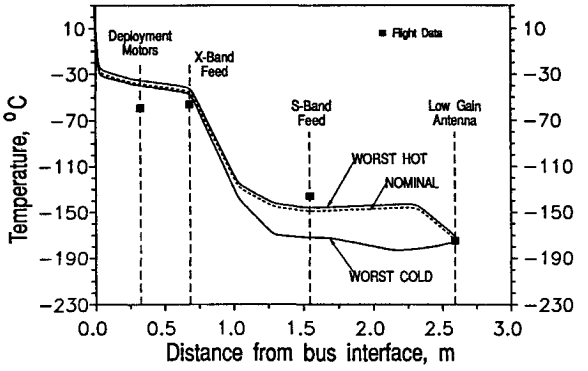

Fig. 8 Cooling turn no. 2 bounding tower temperature prediction and flight data.

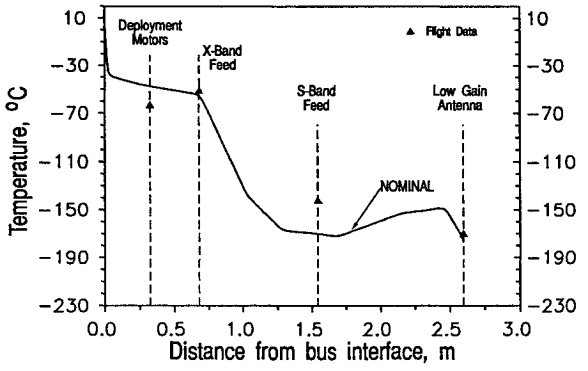

Fig. 9 Cooling turn no. 3 nominal tower temperature prediction and flight data.

antenna temperature predictions for the second cooling turn that are given in Fig. 8.

When the second cooling turn was performed the plasma wave science preamplifier heater was turned off and the dwell time was increased to 50 h after a waiver to permit a higher Probe temperature was granted. Unfortunately, there was no indication of rib release. Comparison between predictions and flight telemetry showed better correlation, however, the midtower temperatures still showed the greatest disparity, as much as a 40°C difference between prediction and flight data (see Fig. 8). Processing the flight data in a similar manner to the first turn, an additional 0.05 ± 0.01 mm of contraction over the first cooling turn was actually achieved. Another cooling turn was planned, but it was decided to schedule the turn where the cooling effect would be most effective. Due to the nature of the trajectory, the spacecraft would reach aphelion (2.27 AU) on Dec. 13, 1991 as shown in Fig. 3. Hence, the turn was scheduled for this time.

The analytical model was not satisfactorily predicting midtower temperatures, which was causing larger-than-actual tower contraction estimates. Prior to the third cooling turn, a modest effort was undertaken to improve midtower predictions. The bus shade was changed from a boundary node to a diffusion node, but when an empirical effective emittance was sized to produce midtower temperatures that agreed with flight data, a non-credible value resulted. The use of typical blanket-effective emittances resulted in temperatures similar to those calculated with the bus shade as a boundary node. Cabling and wave guide conductances were imported from the detailed Harris Corporation thermal model, but only incremental benefits were realized. A decision was made to forego the bus shade and cabling/wave guide conductance improvements since they were not significantly improving tower temperature predictions. Furthermore, investigating the effect that was causing the midtower temperature discrepancy would be difficult and time-consuming since the heat flow is small in the cooling turn environment. Many heat paths that have been neglected in the "hotter" sun-pointed orientation, which was the initial design environment, may no longer be ignored for the cooling turn attitude. A decision was made to use the experience with the two previous cooling turns in concert with the analytical model to develop tower temperature estimates for the third cooling turn.

Precooling turn no. 3 antenna tower predictions were performed, but the temperatures were modified based on the prior two cooling turn flight data to bring the radome area within 20°C of flight data (see Fig. 9). Estimates of tower contraction indicated that between 1.78–1.83 mm would be obtained. When the third cooling turn performed, none of the ribs were freed, and flight data suggested that indeed 1.83 ± 0.01 mm of contraction was achieved. The two previous cooling turn flight data enabled the team to estimate a more realistic tower contraction without an exhaustive effort to improve the analytical model.

Pin Walkout Hypothesis

While the cold soaks of the antenna were performed, the investigation team began to formulate another strategy for freeing the stuck ribs. There was a possibility that the pins would be misaligned with their receptacles by 0.25–0.38 mm. One pin may be pushing up on its receptacle while the other one is pushing down on its receptacle. When the retaining rib spoke was tensioned prior to launch, a locking taper could have been created. The strength of the lock depends on the misalignment and coefficient of friction at the pin/receptacle contact locations. Analysis indicated that the pins might be "walked" out of the taper lock by alternately expanding and contracting the antenna tower by thermal cycling. The warming and cooling of the antenna tower could significantly displace the tower with respect to the ribs, thus shifting the load between the pins. When the tower is warmed, it expands, thereby creating an "upstroke," and similarly a "downstroke" is created by tower cooling. On the upstroke, the load increases on the "lower" pin and it becomes a fulcrum around which the pin pair rotates. When the load on the "upper" pin decreases sufficiently, it slips outward on the receptacle surface until a new load equilibrium point is reached. On the following downstroke, the pin pair reverses roles, and the lower pin slips. Incrementally, the pins reach the point where the lock has been relieved so that the deployment strain energy in the rib overpowers the friction force that restrains it. The hypothesis is based on the pin misalignment and coefficient of friction that are not precisely known.

For the cooling portion of a thermal cycle, the previous 165 deg off-sun attitude was retained, but an optimal warming attitude would have to be determined. Thermal model improvement was necessary since the simplified analytical model could not accurately determine off-sun heat loads. Originally, the rib geometry was developed by constructing three adjacent ribs and then scaling the results to represent all 18 ribs. The spacecraft is spin-stabilized during the cruise phase, and the model was originally utilized for sun-pointed orientations. Such an approximation seemed valid. However, modeling all ribs would be necessary to determine more accurate off-sun heating. Absorbed antenna heating rates for 0–90-deg off-sun pointing were computed with the improved model. However, the molybdenum mesh was neglected as previously assumed. A parametric analysis was performed to determine the tower displacement as a function of off-sun angle for solar distances of 1.0, 1.6, and 2.25 AU (see Fig. 10). An off-sun angle of 50 deg produces maximum tower expansion, however, this angle was not selected for the warming attitude. Shortly after the initial deployment attempt, the spacecraft was turned 45 deg off-sun for 24 h in hopes of warming the antenna near room temperature to relieve pin preload. Since the command sequence for turning the spacecraft 45 deg off-sun had been already developed and the tower expansion difference between off-sun angles of 45 and 50 deg was in-

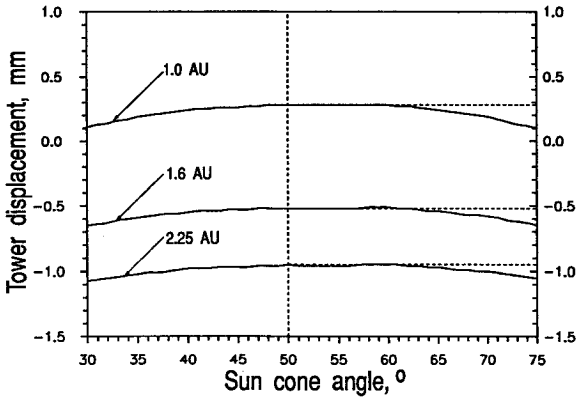

Fig. 10 Predicted tower displacement as a function of off-sun angle for three solar distances.

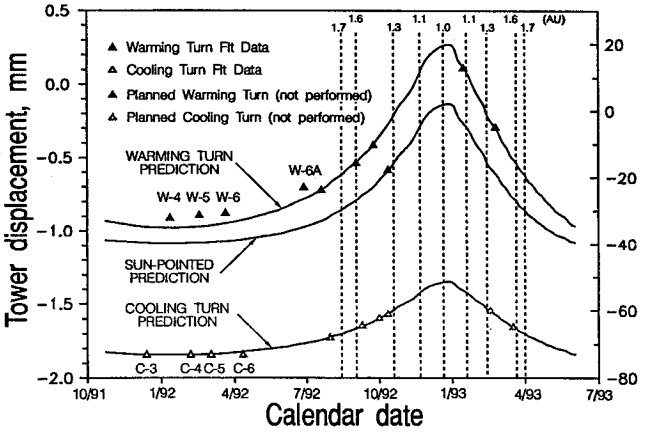

Fig. 11 Predicted and flight data tower displacement as a function of calendar date.

cremental, 45 deg was selected for the warming turn off-sun angle.

Since the pin walking theory is based on the cumulative effect of cycling the antenna, the tower displacements for all previous turns included the return of the antenna to the nominal sun-pointed orientation. Using these displacements and reasonably expected values for pin misalignment and coefficient of friction, computer simulations of pin walking suggested that the ribs might be freed with 6–12 thermal cycles. A thermal cycling regimen was established and antenna tower displacements for the campaign were estimated as functions of the calendar year. Cooling turn results had factored in the previous experiences, however, no such experience base for warming turns had been credibly established. Therefore, warming turn predictions were directly reported. Figure 11 depicts the tower displacement for the proposed thermal cycling strategy. The cooling turn tower displacement error band of ± 0.05 mm is based upon the differences seen between prediction and flight data from the third cooling turn. The error band for the sun-pointed tower displacement predictions is based on the large database of predictions vs flight data, and is ± 0.03 mm. Since an adequate experience base does not exist for warming turns, it is assumed that the warming turn tower displacement error band can be bounded by the cooling turn tower displacement error band (± 0.5 mm). All expectations suggested that the comparison between prediction and flight data for warming turn tower displacement predictions would be substantially better than the cooling turn results. Flight data displacements have an error band of ± 0.01 mm.

The off-sun angles used for thermal cycling were not originally permitted at these solar distances. A great deal of effort was expended to ensure the health and safety of the spacecraft. The 165 deg maneuvering of the spacecraft consumed ~5 kg of propellant, a precious resource.

The three previous cooling turns constituted the first phase of thermal cycling. From January through July of 1992, four additional thermal cycles were performed. The tower displacements suggested by flight data for these cycles are plotted in Fig. 11. There was excellent agreement between the predicted and flight tower temperatures for the warming portion of the cycle. The previous cold soaking experience had led to better predictions for the cold portion of the cycle. The analytical model in concert with flight experience had matured into an accurate tool. After the seventh thermal cycle, dubbed "6A," did not result in rib release, the prospect for freeing any ribs with additional cycling seemed very remote. Either the values for the dominant parameters were too extreme or the mechanism responsible for rib restraint was not well characterized.

Deployment Motor Hammering

The most aggressive action entailed pulsing the deployment motors many times to "hammer" the ball screw. The "hammering" is achieved by cycling power on and off to the deployment motors. Motor pulsing tests conducted with the spare flight high-gain antenna demonstrated that the ball screw rotated beyond the stall point for the motors operating continuously (provided that the motors and gearbox temperatures are greater than approximately 0°C). Estimates indicated that hammering the ball screw would rotate it sufficiently to double the deployment force in one of the ribs. As each rib releases, the deployment forces are concentrated in the remaining stuck ribs. Subsequent hammering could produce larger forces as the number of stuck ribs diminishes.

In preparation for the hammering exercises at 1.0 AU, special activities were performed in July, September, and October of 1992 to characterize the spacecraft thermal response at a 45 off-sun angle, as well as to calibrate and characterize the deployment system. Analysis performed in July 1992 estimated the motor temperature as a function of solar distance for a 45-deg off-sun attitude (see Fig. 12). At that time, three of the four warming turns had been conducted at essentially the same solar distance, hence, the warming turn flight database for the motor consisted of just two cases (1.58 AU and ~2.20 AU). Extrapolation of this data was accomplished by curve-fitting motor temperatures for the sun-pointed condition and off-setting the sun-pointed temperatures by analytically predicted temperature differences predicted between sun-point and 45 deg off-sun.[4]

The spacecraft had not been pointed 45 deg off-sun for lengthy durations inside of 1.58 AU. Concerns were expressed that certain spacecraft elements may overheat. A thermal characterization effort was performed to ensure the thermal health of the spacecraft during the 45-deg off-sun turn at 1.0

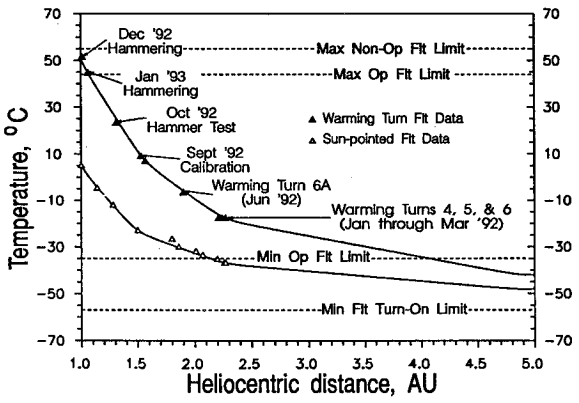

Fig. 12 Predicted and flight deployment motor temperature as a function of solar distance.

Table 2 Summary of near Earth-2 flyby tower displacement estimates

Solar distance, AU	Sun-pointed tower Δl, mm	45-deg off-sun tower Δl, mm
0.986	−0.11	0.29
1.03	−0.19	0.21
1.07	−0.25	0.13
1.10	−0.29	0.08

Note: $\Delta l > 0$ indicates tower expansion and $\Delta l < 0$ indicates tower contraction.

AU. In concert with the overall effort, a contingency analysis was undertaken to determine if more benign off-sun angles could be considered with minor impact to hammer effectiveness. The 45-deg off-sun estimates showed that the deployment motors would attain 51°C at 1.0 AU. Results of this study demonstrated that the motors would achieve 44 and 49°C for off-sun angles of 20 and 30 deg, respectively at 1.0 AU. These angles would be acceptable alternatives for warming the motors above room temperature.

In October 1992 and at a solar distance of 1.30 AU, the spacecraft was turned 45 deg off-sun for about 48 h and the deployment motors were pulsed on and off a few times. Flight data was in excellent agreement with the motor temperature estimates (see Fig. 12). In addition, there were no adverse thermally induced spacecraft problems, therefore, the off-sun warming angle of 45 deg was used.

The motor hammering provided a means to increase rib deployment forces. Since the motor hammering activities were scheduled for Galileo's final Earth flyby, tower expansion would be significant. There was a possibility that the rib-binding mechanism may abate with increasing tower expansion and free the ribs as the spacecraft approached 1.0 AU. Additionally, tower displacement analyses were performed to assist the Earth flyby planning. The flyby solar distance was 0.986 AU and hammering activities were performed at 1.03, 1.07, and 1.10 AU. The thermal model predictions that produced Fig. 11 were changed slightly using flight data extrapolations from the first warming turn at 1.58 AU. The predicted tower displacements for sun-pointed and 45 deg off-sun are summarized in Table 2. As previously stated, tower displacement prediction error bands are ± 0.03 and ± 0.05 mm, respectively for sun-pointed and 45 deg off-sun. Tower displacements at 1.10 AU were determined to be 0.18 and 0.20 mm less than 0.986 AU for sun-pointed and 45 deg off-sun, respectively.

From late-December 1992 to mid-January 1993, the deployment motors were pulsed over 13,000 times while the spacecraft was 45 deg off-sun. Again, flight data of motor temperature was in excellent agreement with prehammering estimates (see Fig. 12). Although flight telemetry indicated that the antenna rib configuration had changed, the stuck ribs had not been freed. By the end of February 1993, the investigative team was dissolved, and the Project proceeded with the implementation of new capabilities to perform the mission with the low-gain antenna in accordance with plans established in April 1992. At least 70% of the mission objectives will be achievable using the low-gain antenna.

Concluding Remarks

An intensive effort was performed to thermally characterize the antenna and the spacecraft. Initially, correlation for the cooling turns was lacking. However, with additional flight experience, the predictive capability improved significantly without an exhaustive overhaul of the thermal model. The analytical model, itself, has evolved over the course of time, where it has demonstrated good agreement with flight data especially for warming turns and sun-pointed attitudes (within 5°C). Flight experience was used in tandem with the analytical model to provide satisfactory temperature estimates for cooling turns.

Acknowledgments

The research described in this article was carried out by the Jet Propulsion Laboratory, California Institute of Technology, under a contract with NASA. The thermal support for the high-gain antenna recovery effort could not have been responsive if not for the dedicated work of Art Avila, Rodney Badin, Jerry Millard, and Jesse Smith in the Galileo Mission Operations Area. Wes Anderson, Robert Giampaoli, and Keith Novak assisted with the high-gain antenna thermal model improvements. Additional recognition is due to Gary Kinsella, Bill Ledeboer, Virgil Mireles, and Bob Miyake who made significant contributions to the investigative thermal team. The authors would like to express their gratitude to Matt Landano and Bill O'Neil for providing their descriptions of the high-gain antenna recovery actions and editing the manuscript. We would also like to thank Gary Coyle, Galileo High-Gain Antenna Cognizant Engineer, for reviewing the manuscript.

References

[1]O'Neil, W. J., "Project Galileo Mission Status," International Astronautical Federation Paper 91-468, Oct. 1991.

[2]O'Neil, W. J., Ausman, N. E., Jr., Johnson, T. V., and Landano, M. R., "Galileo Completing VEEGA—A Mid-Term Report," International Astronautical Federation Paper 92-0560, Aug. 1992.

[3]Reeve, R. T., "Thermal Redesign of the Galileo Spacecraft for a VEEGA Trajectory," *Journal of Spacecraft and Rockets*, Vol. 28, No. 2, 1991, pp. 130–138.

[4]Tsuyuki, G., "Galileo High Gain Antenna Motor Temperature as a Function of Heliocentric Distance," Jet Propulsion Lab., 3548-CAS-92-090, Pasadena, CA, June 1992.